JOURNAL OF MATERIALS SCIENCE 7 (1972) 888-894

Ostwald ripening during solidification of nondendritic spherical structures

N. J. WHISLER*, T. Z. KATTAMIS
Department of Metallurgy, Institute of Materials Science, University of Connecticut, Storrs, Connecticut, USA

A theoretical model was introduced for the study of Ostwald ripening during solidification of the nondendritic spherical structure observed in Mg-Zn alloys grain-refined with Zr. This model assumed that: (1) particles are spherical; (2) each particle receives during solidification a mass increment proportional to its volume fraction with respect to the total volume of the particles in the system; (3) the Scheil equation applies. Experimental results agreed with analytical predictions on the time variation of the total solid-liquid interface area per unit volume and of the relative number of particles per unit volume.

1. Introduction

It is well known [1-4] that the microstructure of cast magnesium-zinc alloy grain-refined with zirconium consists of spherical nondendritic grains that exhibit spherical coring and are partially or totally surrounded by non-equilibrium secondary phase, Mg_7Zn_3. Grain size increases with distance from the chill, whereas the number of grains per unit volume decreases. The important role played by Ostwald ripening in the establishment of final grain size in such alloys has been experimentally illustrated [1] both during normal solidification and during isothermal holding of solid in presence of liquid. The purpose of the present study is to introduce a model describing ripening during solidification of a grain-refined magnesium-zinc alloy and to compare analytical predictions of the model with experimental results.

2. Experimental procedure

Two plates (9 × 6 × 0.75 in. thick) of grain-refined Mg-5.1 % Zn-0.6 % Zr alloy were sand-cast and end-chilled using standard magnesium melting and casting techniques. Six specimens were taken, placed in small steel crucibles, remelted under flux and cooled in a programmed furnace at a constant rate of 100°C/h. One sample was removed from the controlled cooling environment and water-quenched at each of six different time intervals during solidification (5 sec from initiation of solidification, 2×10^3, 4×10^3, 6×10^3, 8×10^3 and 10^4 sec). Metallographic specimens were prepared and etched using a mixture of ethylene glycol and aqueous solution of oxalic acid. Structures observed were analogous to those previously reported [1]. Photomicrographs were taken and the total surface area of spheres per unit volume, S_V(mm^2/mm^3) was determined using the following relationship [5]:

$$S_V = 2\bar{N}_L \quad (1)$$

where: $\bar{N}_L$ = average number of interface intersections per unit length of test line (mm^{-1}). For each photomicrograph many random test lines were used for a more accurate calculation of S_V.

The number of spherical particles per unit volume, N_V, was determined using the Schwartz-Saltykov analysis [6]. The same experiment was repeated with five specimens cooled at 9°C/h and five other specimens held isothermally at 615°C. For these specimens solidification was interrupted by quenching 5, 2×10^3 4, $\times 10^3$, 6×10^3 and 8×10^3 sec after initiation.

3. Analytical coarsening model

A theoretical model was developed to describe coarsening of spheres during solidification. Coarsening will be analysed herein, firstly for a system of two spherical particles held isotherm-

*Now with the Bureau of Mines, Reno, Nevada 89502, USA.

ally in presence of liquid, secondly for a system of several spherical particles held isothermally in presence of liquid and finally for a system of several spherical particles during continuous freezing.

3.1. System of two spherical particles held isothermally in presence of liquid

Assume an isothermal system consisting of two spherical particles of primary Mg-rich α-phase of different radii, surrounded by melt.

The solute balance for a dissolving particle [7, 8] at temperature T can be written as:

$$C_L^a(1-K)\rho\, 4\pi a^2 \frac{da}{dt} = -D\rho\, 4\pi r^2 \frac{dC_L}{dr} \quad (2)$$

where: C_L^a = concentration of solute in the liquid at temperature T in equilibrium with a surface of radius a, wt %, C_L = concentration of solute in the liquid at distance r, wt %, K = equilibrium partition ratio, ρ = density, g/cm³, a = radius of smaller particle, cm, t = time, sec, D = diffusivity of solute in liquid, cm²/sec, r = distance from centre of particle, cm. Assuming $C_L^a \simeq C_L$ [9] and rearranging:

$$-\frac{C_L(1-K)a^2}{Dr^2}\left(\frac{da}{dt}\right) dr = dC_L \quad (3)$$

Integrating between $r = a$ and $r = \infty$

$$-\int_a^\infty \frac{C_L(1-K)a^2}{Dr^2}\left(\frac{da}{dt}\right) dr = \int_{C_L^a}^{C_L^\infty} dC_L \quad (4)$$

$$\frac{da}{dt} = \frac{D}{C_L(1-K)a}(C_L^\infty - C_L^a) \quad (5)$$

Assuming [7, 8] that:

$$C_L^\infty - C_L^a \cong C_L^R - C_L^a \quad (6)$$

$$C_L^\infty - C_L^a = \frac{\sigma T}{mH}\left[\frac{1}{R} - \frac{1}{a}\right] \quad (7)$$

where C_L^R = concentration of solute in the liquid at temperature T in equilibrium with a surface of radius R, wt %, R = radius of the larger particle, cm, H = volumetric heat of fusion, cal/cm³, m = slope of the liquidus, K/%, σ = solid-liquid interface energy, cal/cm².

Therefore:

$$\frac{da}{dt} = \frac{D\sigma T}{C_L(1-K)mH}\left[\frac{1}{R} - \frac{1}{a}\right]\frac{1}{a} \quad (8)$$

Equation (8) gives the rate of disappearance of the smaller particle.

The total volume of solid, V, remains constant during the isothermal holding. Hence:

$$\frac{dV}{dt} = 0 \quad (9)$$

where:

$$V = \frac{4\pi}{3}(a^3 + R^3)$$

From (9) it follows that:

$$\frac{dR}{dt} = -\frac{a^2}{R^2}\left(\frac{da}{dt}\right) \quad (10)$$

$$\frac{dR}{dt} = \frac{-aD\sigma T}{R^2 C_L(1-K)mH}\left[\frac{1}{R} - \frac{1}{a}\right] \quad (11)$$

By changing variable names from a and R to r_1 and r_2:

$$\frac{dr_1}{dt} = -\frac{D\sigma T}{C_L(1-K)mHr_1}\left[\frac{1}{r_1} - \frac{1}{r_2}\right] \quad (12)$$

$$\frac{dr_2}{dt} = -\frac{r_1 D\sigma T}{r_2^2 C_L(1-K)mH}\left[\frac{1}{r_2} - \frac{1}{r_1}\right], r_1 < r_2 \quad (13)$$

The general expression for the rate of change of the radius of a sphere in this system can then be written as:

$$\frac{dr_i}{dt} = -\frac{D\sigma T}{C_L(1-K)mHr_i}\left[\frac{1}{r_i} - \frac{1}{r_j}\right]\mathcal{H}(r_j - r_i) + \frac{-r_j D\sigma T}{r_i^2 C_L(1-K)mH}\left[\frac{1}{r_i} - \frac{1}{r_j}\right]\mathcal{H}(r_i - r_j) \quad (14)$$

where:

$\mathcal{H}(\alpha - \beta) = 0$, for $\alpha < \beta$
$\mathcal{H}(\alpha - \beta) = 1$, for $\alpha > \beta$
(Heaviside function)

3.2. System of several spherical particles held isothermally in presence of liquid

Consider now a system of $n > 2$ spherical particles and assume that the coarsening relationship between any two particles i and j is still given by expression (14). The radii of these two particles will obviously be influenced by the other $(n-2)$ particles; the coarsening relationship will exist between particle i and any other particle in the system and between particle j and any other particle in the system.

This can be written as:

$$\frac{dr_i}{dt} = \sum_{\substack{j=1 \\ j \neq i}}^{n} \frac{dr_{i(j)}}{dt} \quad (15)$$

where:

$$\frac{dr_{i(j)}}{dt} = \text{the component of } \frac{dr_i}{dt}$$

caused by the jth particle ($j \neq i$), as given by (14)

Hence:

$$\frac{dr_i}{dt} = \sum_{\substack{j=1 \\ j \neq i}}^{n} \left\{ \frac{-D\sigma T}{C_L(1-K)mHr_i} \left[\frac{1}{r_i} - \frac{1}{r_j}\right] \mathscr{H}(r_j - r_i) + \frac{-D\sigma T r_j}{C_L(1-K)mHr_i^2} \left[\frac{1}{r_i} - \frac{1}{r_j}\right] \mathscr{H}(r_i - r_j) \right\} \quad (16)$$

The radius of the sphere i as a function of time is then:

$$r_i = r_0 + \int_0^t \left(\frac{dr_i}{dt}\right) dt \quad (17)$$

3.3. System of several spherical particles during continuous freezing

The cooling process may be subdivided into a large number of steps, each one consisting of an isothermal hold of duration Δt sec followed by an instantaneous cooling (quenching) of ΔT°C. Coarsening operates during the isothermal hold and solidification growth during quenching.

Expression (17) may be written as:

$$r_i = r_0 + \lim_{\substack{\Delta t_k \to 0 \\ k \to \infty}} \sum_{t=0}^{t_k} \frac{dr_{ik}}{dt} \cdot \Delta t_k \quad (18)$$

where

$$\frac{dr_{ik}}{dt} = \frac{dr_i}{dt}$$

calculated at the kth time step, assuming that among the various parameters appearing in expression (16): σ, D and H are constant with temperature and time, C_L, K, m vary with temperature and time. Δt_k length of kth time step.

The surface-to-volume ratio at any time $t = \sum_{k=1}^{k} \Delta t_k$ depends on both solidification growth and coarsening and is given by:

$$S_v = \frac{\sum_{i=1}^{n} 4\pi r_i^2}{\sum_{i=1}^{n} \frac{4}{3}\pi r_i^3} \quad (19)$$

The rate of change of S_v due to coarsening alone,

$$\left(\frac{dS_v}{dt}\right)_c$$

may be obtained from (19) assuming constant volume for each time step. Volume changes between time steps. Thus:

$$\left(\frac{dS_v}{dt}\right)_c = \frac{\sum_{i=1}^{n} 8\pi r_i \left(\frac{dr_i}{dt}\right)_c}{\sum_{i=1}^{n} \frac{4}{3}\pi r_i^3} \quad (20)$$

where c = indicates contribution of coarsening to the variation of a parameter or function.

Hence:

$$(\Delta S_v)_c \cong \lim_{\substack{\Delta t_k \to 0 \\ k \to \infty}} \sum_{k=1}^{k} \frac{\sum_{i=1}^{n} 8\pi r_{ik} (\Delta r_{ik})_c}{\sum_{i=1}^{n} \frac{4}{3}\pi r_{ik}^3} \quad (21)$$

where $(\Delta S_v)_c$ = change of S_v occurring during time t, due to coarsening, k = number of time steps, $(\Delta r_{ik})_c$ = change in r_i due to coarsening at the kth time step

$$\left(\frac{dr_i}{dt}\right)_c \cdot \Delta t_k$$

The change in r_i due to normal solidification growth which occurs at time t during the time interval Δt_k may be expressed by:

$$(\Delta r_{ik})_g = \mathscr{F}[(\Delta M/\Delta t)(\Delta t_k/\rho A)] \quad (22)$$

where $(\Delta M/\Delta t)$ = rate of change of mass of solid at time t due to solidification, ρ = density of the solid, a function of temperature and composition, A = an appropriate area expression, g = indicates contribution of coarsening to the variation of a parameter of function.

It will be assumed that: (1) each particle receives during solidification a mass increment proportional to its volume fraction relatively to the total volume of all the particles; (2) the Scheil equation applies to this system. Hence, the rate of change of weight fraction solid,

$$\frac{df_s}{dt},$$

may be deduced [10, 11] from:

$$f_s = 1 - \left[\frac{T_M - T_L}{T_M - T}\right]^{1/1-k} \quad (23)$$

where f_s = weight fraction solid, T_L = equilibrium liquidus temperature, T_M = melting temperature of pure solvent. Through time derivation:

$$\frac{df_s}{dt} = \left(\frac{1}{1-k}\right)\frac{[T_M - T_L]^{1/1-k}}{[T_M - T]^{2-k/1-k}}\left(\frac{dT}{dt}\right) \quad (24)$$

The mass of solid in the volume element* [11] at a given time, M, is given by:

$$M = M_T \cdot f_s \quad (25)$$

where M_T = total mass of the volume element. Hence:

$$\left(\frac{\Delta M}{\Delta t}\right) = M_T\left(\frac{1}{1-K}\right)\frac{[T_M - T_L]^{1/1-k}}{[T_M - T]^{2-k/1-k}}\left(\frac{\Delta T}{\Delta t}\right) \quad \ldots . (26)$$

The explicit form of (22) is:

$$(\Delta r_{ik})_g = \frac{M_T\left(\frac{1}{1-K}\right)\frac{[T_M - T_L]^{1/1-k}}{[T_M - T]^{2-k/1-k}}\left(\frac{\Delta T}{\Delta t}\right)\cdot\frac{r_i^3}{\sum_{i=1}^{n} r_i^3}\cdot\Delta t_k}{4\pi\rho r_i^2} \quad \ldots . (27)$$

Thus, the radii of all the spheres of the system can be calculated at the end of any number of time steps, hence at any time, t, by evaluating expressions (16) and (18) by means of a digital computer. These radii can then be adjusted to take into account normal solidification growth during the quenching steps by means of expression (27). The system can therefore be described at any time. S_v may be calculated using expression (19). The change of S_v which occurs during a given time due to coarsening, $(\Delta S_v)_c$ may be determined from expression (21) using a digital computer.

At a given time t after initiation of solidification:

$$S_v = S_{vo} + (\Delta S_v)_c + (\Delta S_v)_g \quad (28)$$

where S_{vo} = initial S_v at the onset of solidification, $(\Delta S_v)_g$ = change of S_v occurring during time t due to solidification growth. $(\Delta S_v)_g$ may be calculated from (28) where all other terms are known.

The preceding analysis was applied to the series of specimens cooled at 100°C/h. As initial particle configuration was taken that of the specimen that was cooled at this rate and was water quenched 5 sec after initiation of solidification. By successively polishing down the specimen and metallographically examining various surfaces it was established that a given particle is surrounded by an average of 18 other particles. Thus, it was assumed that a given particle interacts with 18 other particles. A typical radii distribution used in this computation was: $r_1 = 0.0069$ mm, $r_2 = 0.0116$ mm, $r_3 = 0.00139$ mm, $r_4 = 0.0186$ mm, $r_5 = 0.0198$ mm, $r_6 = 0.0205$ mm, $r_7 = 0.0215$ mm, $r_8 = 0.0223$ mm, $r_9 = 0.0233$ mm, $r_{10} = 0.0278$ mm, $r_{11} = 0.0305$ mm, $r_{12} = 0.0347$ mm, $r_{13} = 0.0395$ mm, $r_{14} = 0.0442$ mm, $r_{15} = 0.0485$ mm, $r_{16} = 0.0533$ mm, $r_{17} = 0.0580$ mm, $r_{18} = 0.0620$ mm, $r_{19} = 0.0671$ mm. The corresponding $S_{vo} = 60.548$ mm^{-1}. Other data used in the calculation were [13-15]: $D = 1.0 \times 10^{-3}$ mm^2/sec, $m = -6.160$ K/% Mg, $K = 0.168$, $\sigma = 0.61 \times 10^{-8}$ cal/mm^2, $H = -0.131$ cal/mm^3 $\rho_{Mg} = 1.74$ g/mm^3, $\rho_{Zn} = 7.14$ g/mm^3; ρ_{alloy} was computed for each composition versus time, C_L was deducted from the phase diagram: $C_L = (650\text{-}T)/6.10$. The calculations were conducted as previously analysed. They were repeated for other cooling rates: 9, 18 and 36°C/h and for an isothermal holding experiment conducted at 615°C ($f_s \simeq 0.2$) using in each case the appropriate initial structure.

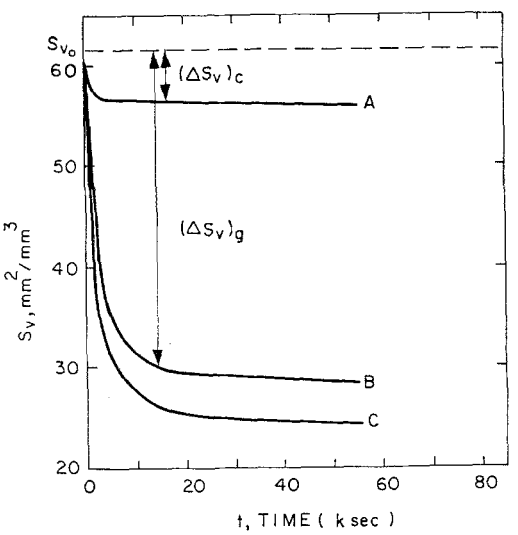

Figure 1 Solid-liquid interfacial area per unit volume, S_v, versus time. Mg-5.1 wt % Zn-0.6 wt % Zr alloy solidified at 18°C/h before quenching. (A) Contribution of Ostwald ripening, (B) contribution of normal solidification growth, (C) total.

*In this alloy each sphere that survives dissolution grows into a polyhedron at the end of solidification [4]. This polyhedron can be roughly approximated by the Voronoi polyhedron and has a volume equal to that of the Dirichlet sphere [12]. It has been taken herein as the volume element. Thus, at a given time f_s is the weight of the growing sphere divided by the weight of this polyhedron.

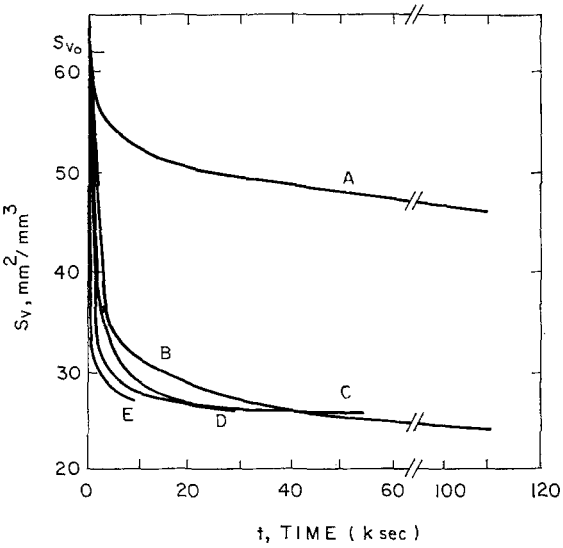

Figure 2 Solid-liquid interfacial area per unit volume, S_v, versus time for various cooling rates. Mg-5.1 wt% Zn-0.6 wt% Zr alloy. (A) isothermal, (B) 9°C/h, (C) 18°C/h, (D) 36°C/h, (E) 100°C/h.

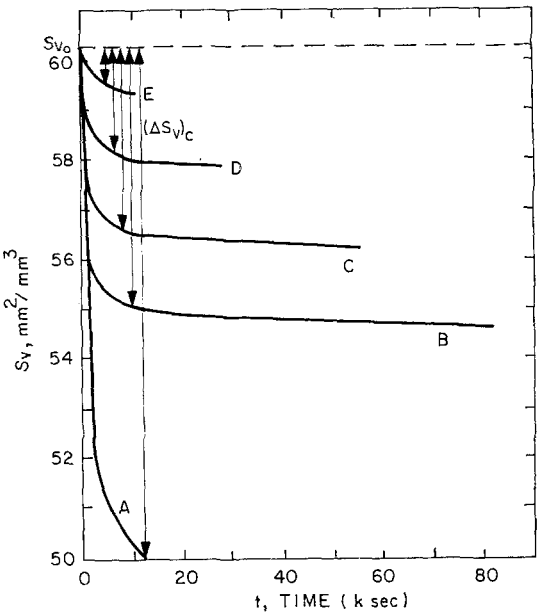

Figure 3 Contribution of coarsening to the variation of the solid-liquid interfacial area per unit volume, S_v, versus time. Mg-5.1 wt% Zn-0.6 wt% Zr alloy solidified at: (A) isothermal, (B) 9°C/h, (C) 18°C/h, (D) 36°C/h, (E) 100°C/h.

4. Results and discussion

The variation of total S_v, of the Ostwald ripening component $(\Delta S_v)_c$, and of the normal solidification growth component, $(\Delta S_v)_g$, versus time were analytically calculated for various cooling rates: 0°C/h (isothermal), 9, 18, 36 and 100°C/h. The ratio of the number of particles per unit volume remaining at a given time to the initial number of particles per unit volume, N/N_o, was also calculated for these cooling rates. Fig. 1 illustrates the variation of total S_v, $(\Delta S_v)_c$ and $(\Delta S_v)_g$ versus time for a cooling rate of 18°C/h. Fig. 2 illustrates the variation of total S_v versus

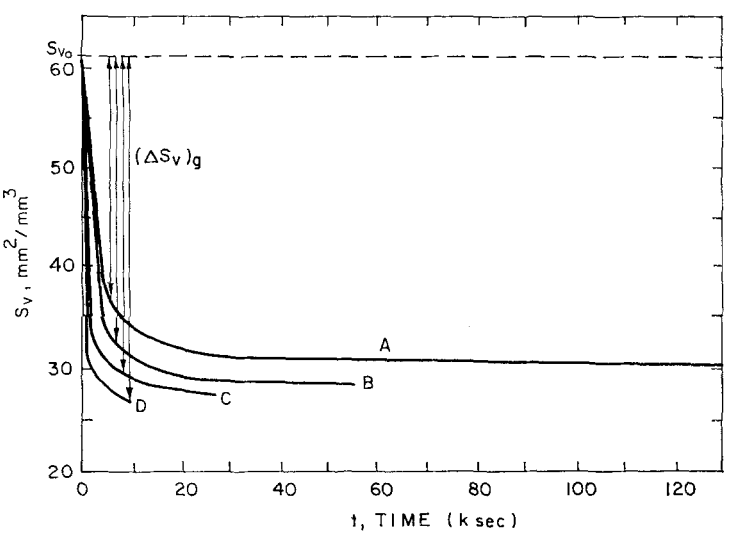

Figure 4 Contribution of normal solidification growth to the variation of the solid-liquid interfacial area per unit volume, S_v, versus time. Mg-5.1 wt% Zn-0.6 wt% Zr alloy solidified at: (A) 9°C/h, (B) 18°C/h, (C) 36°C/h, (D) 100°C/h.

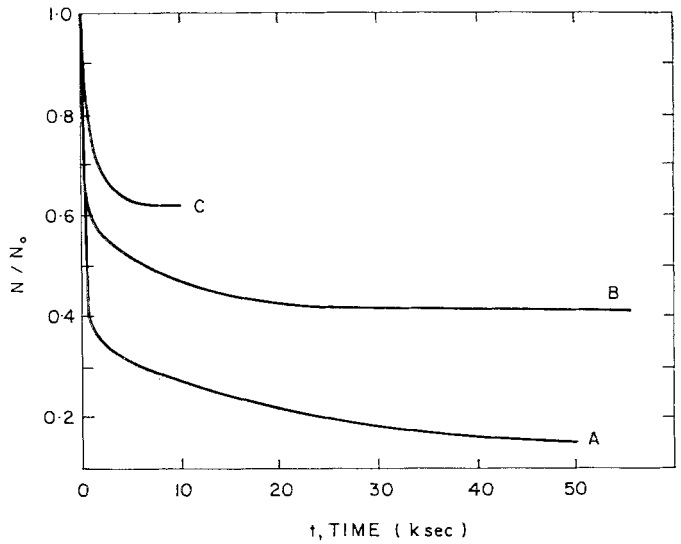

Figure 5 Variation of N/N_0 versus time for various cooling rates. Mg-5.1 wt % Zn-0.6 wt % Zr alloy. (A) 9°C/h, (B) 18°C/h, (C) 100°C/h.

time for various cooling rates. The time variations of the contributions of Ostwald ripening and normal solidification growth to S_V for various cooling rates are plotted in Figs. 3 and 4, respectively. The variation of N/N_0 versus time for various cooling rates is illustrated in Fig. 5.

Experimental values of total S_V versus time t which solidification proceeded before during quenching are reported in Fig. 6 for the isothermal case and for cooling rates of 9 and 100°C/h and compared with the corresponding analytical curves. Experimental values of N/N_0 reported versus time are compared with analytical curves in Fig. 7.

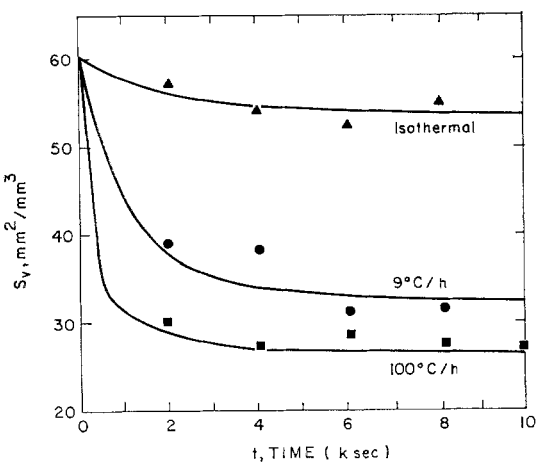

Figure 6 S_V versus time. Mg-5.1 wt % Zn-0.6 wt % Zr alloy held isothermally at 615°C, cooled at 9°C/h, cooled at 100°C/h. Experimental points and analytical curves.

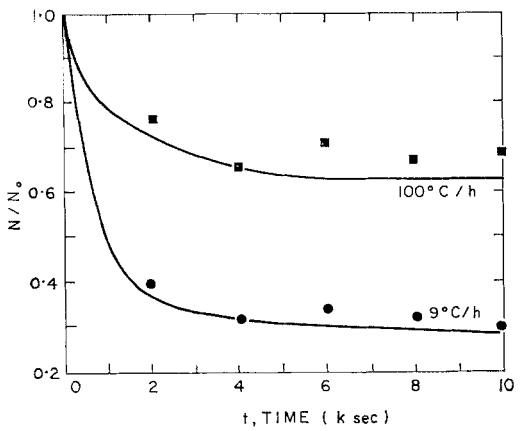

Figure 7 N/N_0 versus time Mg-5.1 wt % Zn-0.6 wt % Zr alloy solidified at 9°C/h and 100°C/h. Experimental points and analytical curves.

Fig. 1 shows that S_V decreases at first rapidly with time and soon levels off. Similar observations are made for both the coarsening and the normal solidification growth contributions. The rate of increase of $(\Delta S_V)_c$ decreases with time, because the temperature decreases with time, whereas liquid concentration and particle radii increase [expressions (16), (18) and (20)]. similarly the rate of increase of $(\Delta S_V)_g$ decreases with time, because the fraction solid deposited per unit time decreases with decreasing tempera-

ture or increasing time, as predicted by expression (26).

The direct contribution of coarsening to the variation of S_V, $(\Delta S_V)_c$, is smaller than that of normal solidification growth, $(\Delta S_V)_g$. However, coarsening is responsible for the removal of fine particles from the system and thus enhances the contribution solidification growth, because the newly solidified material is then deposited on fewer particles. Fig. 2 shows that for a given time S_V consistently decreases with increasing cooling rate. This is because the total amount of material deposited increases with decreasing temperature. Fig. 3 shows that the contribution of Ostwald ripening to S_V decreases as expected, with increasing cooling rate. The intersection of curves in Fig. 2 is presumably due to the fact that for a given time the contribution of coarsening increases with decreasing cooling rate, whereas that of normal solidification growth decreases.

The variation of N/N_0 versus time, Fig. 5, becomes more significant for lower cooling rates. This is because (1) the amount of solid deposited through solidification growth for a given time is smaller for lower cooling rates and the time required for particle disappearance through dissolution is affected less; (2) for lower cooling rates coarsening operates for a longer time.

The solidification model introduced herein agrees reasonably well with experimental observations, Figs. 6 and 7. The analytical curves were found to be rather insensitive to any reasonable variation of initial particle distribution. The assumption that the change in mass of a particle is proportional to its mass or volume, or that each particle solidifies independently is then realistic.

Acknowledgement

This work was jointly sponsored by Air Force Office of Scientific Research Contract No F44620-69-C-0011, by a University of Connecticut Research Foundation Grant, and by a National Science Foundation Grant GJ-9 to the University of Connecticut Computer Center.

References

1. T. Z. KATTAMIS, U. T. HOLMBERG, and T. Z. KATTAMIS, *J. Inst. Metals* **95** (1967) 343.
2. E. F. EMLEY, "Principles of Magnesium Technology" (Pergamon Press, New York, 1966).
3. A. K. BHAMBRI and T. Z. KATTAMIS, *Scripta Met.* **5** (1971) 53.
4. *Idem, Met. Trans.* **2** (1971) 1869.
5. C. S. SMITH and L. GUTTMAN, *Trans. AIME*, **197** (1953) 81.
6. S. A. SALTYKOV, "Stereometric Metallography", 2nd ed. (Metallurgizdat, Moscow, 1958) p. 446.
7. G. W. GREENWOOD, *Acta Metallurgica* **4** (1956) 243.
8. C. WAGNER, *Z. Elektrochem.* **65** (1961) 581.
9. T. Z. KATTAMIS, J. M. COUGHLIN, and M. C. FLEMINGS, *Trans. AIME*, **239** (1967) 1504.
10. E. SCHEIL, *Z. Metalk.* **34** (1942) 70.
11. H. D. BRODY and M. C. FLEMINGS, *Trans. AIME*, **236** (1966) 615.
12. A. J. ARDELL, *Acta Metallurgica* **20** (1972) 61.
13. C. J. SMITHELLS, "Metals Reference Book", 3rd ed., Vol. 2 (Butterworth, Washington, 1962) p. 589.
14. "Handbook of Chemistry and Physics", 39th edition, Chemical Rubber Publishing Co, 1958.
15. T. Z. KATTAMIS, current investigation, Department of Metallurgy, University of Connecticut, Storrs, Connecticut.

Received 20 January and accepted 10 February 1972.